

Association between in-scanner head motion with cerebral white matter microstructure: A multiband diffusion-weighted MRI study

Diffusion-weighted Magnetic Resonance Imaging (DW-MRI) has emerged as the most popular neuroimaging technique used to depict the biological microstructural properties of human brain white matter. However, like other MRI technique, traditional DW-MRI data remains subject to head motion artifacts during scanning. For example, previous studies have indicated that, with traditional DW-MRI data, head motion artifacts significantly affect the evaluation of diffusion metrics. Actually, DW-MRI data scanned with higher sampling rate are important for accurately evaluating diffusion metrics because it allows for full-brain coverage through the acquisition of multiple slices simultaneously and more gradient directions. Here, we employed a publicly available multiband DW-MRI dataset to investigate the association between motion and diffusion metrics with the standard pipeline, tract-based spatial statistics (TBSS). The diffusion metrics used in this study included not only the commonly used metrics (i.e., FA and MD) in DW-MRI studies, but also newly proposed inter-voxel metric, local diffusion homogeneity (LDH). We found that the motion effects in FA and MD seems to be mitigated to some extent, but the effect on MD still exists. Furthermore, the effect in LDH is much more pronounced. These results indicate that researchers shall be cautious when conducting data analysis and interpretation. Finally, the motion-diffusion association is discussed.

1 **Title:** Association between In-scanner Head Motion and Cerebral White Matter Microstructure: A Multiband
2 Diffusion-weighted MRI study

3 **Running head:** Head Motion and White Matter Microstructure

4 **Authors:** Xiang-zhen Kong^{1,2}

5 **Affiliation:** ¹ State Key Laboratory of Cognitive Neuroscience and Learning & IDG/McGovern Institute for
6 Brain Research, Beijing Normal University, Beijing, 100875, China; ² Center for Collaboration and Innovation
7 in Brain and Learning Sciences, Beijing Normal University, Beijing, 100875, China.

8 **Correspondence Author:**

9 Xiang-zhen Kong; 2nd Floor, Brain Imaging Center, 19 Xijiekouwai St, Haidian District, Beijing 100875,
10 China. E-mail: kongxiangzheng@gmail.com

11 **Abstract**

12 Diffusion-weighted Magnetic Resonance Imaging (DW-MRI) has emerged as the most popular neuroimaging
13 technique used to depict the biological microstructural properties of human brain white matter. However, like
14 other MRI technique, traditional DW-MRI data remains subject to head motion artifacts during scanning. For
15 example, previous studies have indicated that, with traditional DW-MRI data, head motion artifacts
16 significantly affect the evaluation of diffusion metrics. Actually, DW-MRI data scanned with higher sampling
17 rate are important for accurately evaluating diffusion metrics because it allows for full-brain coverage through
18 the acquisition of multiple slices simultaneously and more gradient directions. Here, we employed a publicly
19 available multiband DW-MRI dataset to investigate the association between motion and diffusion metrics with
20 the standard pipeline, tract-based spatial statistics (TBSS). The diffusion metrics used in this study included not
21 only the commonly used metrics (i.e., FA and MD) in DW-MRI studies, but also newly proposed inter-voxel
22 metric, local diffusion homogeneity (LDH). We found that the motion effects in FA and MD seems to be
23 mitigated to some extent, but the effect on MD still exists. Furthermore, the effect in LDH is much more
24 pronounced. These results indicate that researchers shall be cautious when conducting data analysis and
25 interpretation. Finally, the motion-diffusion association is discussed.

26 **Keywords:** Head Motion; White Matter; Microstructure

27 Introduction

28 Diffusion-weighted MRI (DW-MRI) has become one of the most popular MRI techniques in brain research, as
29 well as in clinical practice. One key application of DW-MRI is diffusion tractography which can be used for the
30 visualization of white matter (WM) tracts (Golby et al. 2011) and construction of the brain neuroanatomical
31 connectome (Gong et al. 2009). Also, it has become a convenient tool for deriving regional measures of
32 diffusivity and anisotropy. These metrics are believed to reflect biological microstructural properties of the
33 white matter, and have been extensively applied as biological markers for studying WM under normal and
34 clinical conditions (Johansen-Berg 2010; Le Bihan 2003; Le Bihan et al. 2001; Travers et al. 2012).

35 However, like other MRI technique, DW-MRI remains subject to specific biological factors (e.g.,
36 temperature), uncertainty from the scanner (e.g., machine SNR, field shim) and, in particular, motion artifacts.
37 Thus, movement of the head during scanning is undesirable, since it not only displaces the brain matter in space
38 but also interferes with the readout of MR signals. Indeed, recent studies have discovered that head motion may
39 introduce unwanted biases. Ling and his colleagues have shown that head motion is associated with both
40 fractional anisotropy (FA) and mean diffusivity (MD) (the effect is greater for MD) (Ling et al. 2012). A recent
41 study have also found group differences in head motion can induce group differences in white matter tract-
42 specific diffusion metrics, and such effects can be more prominent in some specific tracts than others (Yendiki
43 et al. 2013). However, these studies on head-motion artifacts have employed traditional DW-MRI data with
44 relatively low sampling rate (e.g., 9 s) and hence few number of gradient directions (e.g., $n = 30$). In fact,
45 previous works have indicated that more unique sampling directions may decrease bias of diffusion metrics
46 (e.g., FA and MD) (Landman et al. 2007; Tijssen et al. 2009). Recently, several promising imaging techniques
47 have been proposed, including MR-encephalography (Zahneisen et al. 2011) and multiband echo planar
48 imaging (Moeller et al. 2010). Using the multiband scanning protocol, full-brain coverage is allowed through
49 the acquisition of multiple slices simultaneously. Hence, additional gradient directions can be acquired in the
50 same scan duration without loss in spatial resolution. Both of the advantages appear to result in evaluating
51 diffusion metrics more accurately, but little is known about the head motion effects on diffusion metrics from
52 the multiband dataset.

53 Here, the primary aim was therefore to investigate the relationship between head motion and diffusion
54 metrics estimated from the multiband dataset. In this study, we examined the two tensor-based metrics most
55 typically reported (i.e., FA and MD). Given the fact that they only reflect diffusion properties solely within the
56 voxel, we also examined a newly proposed model-free inter-voxel metric, referred to as local diffusion

57 homogeneity (LDH) (Gong 2013). We hypothesized that motion effects would be mitigated in the multiband
58 DW-MRI data. It has been suggested that head motion alters the measure of diffusion metrics even after motion
59 and eddy current correction (Ling et al. 2012; Tijssen et al. 2009; Yendiki et al. 2013), and that it may also
60 provide information regarding neuronal processing (Yan et al. 2013a; Yan et al. 2013b). Moreover, LDH is a
61 recently proposed metrics and has not been fully validated yet (Gong 2013). In addition, unlike FA and MD,
62 LDH directly depends on the raw diffusivity series without assuming a prior diffusion model (Gong 2013).
63 Therefore, we also hypothesized that the association between head motion and LDH would be quite different to
64 the tensor-based metrics, and may be more sensitive to motion artifacts. We tested these hypotheses by (1)
65 confirming the test-retest reliability of both diffusion metrics and head motion across scan sessions, and (2) by
66 examining the relationship between the averaged diffusion metrics and head motion. We also examined the
67 relationship in each scan session.

68 **Materials and Methods**

69 **Dataset**

70 The dataset used in this study was from the NKI-RS Multiband Imaging Test-Retest Pilot Dataset (Mennes et
71 al. 2012). There were 20 participants (34.3 ± 14.0 years). For each participant, the DW-MRI scans were
72 performed twice (session 1 and session 2), around one week apart. Diffusion weighted images were collected a
73 standard pulse sequence with 2-mm-thick axial slices and 137 directions: TE 85 ms; TR 2400 ms; b value, 1500
74 s/mm²; flip angle, 90°.

75 **Image Processing**

76 DW-MRI images were processed with FMRIB's Software Library (FSL, <http://www.fmrib.ox.ac.uk/fsl>). Non-
77 brain tissue was removed using the Brain Extraction Tool (BET) with a fractional intensity threshold of 0.2, and
78 then raw DW images were affinely registered to the nonDW image, to partially correct for the effects of motion
79 and eddy currents. Then, by fitting a tensor model at each voxel using DTIFit from the FSL (Smith et al. 2004),
80 we obtained the fractional anisotropy (FA) and mean (MD) diffusivity, used in subsequent TBSS analysis
81 (Smith et al. 2006; Smith et al. 2007).

82 To compare between subjects, the TBSS framework was used. In detail, first, we non-linearly aligned the
83 individual FA maps to FSL's standard 1 mm isotropic FA template (FMRIB58_FA) and averaged them to
84 generate a study specific mean FA map. Next, voxels with an FA > 0.2 in the mean FA map were masked out,
85 and the remainder was thinned to create a white matter "skeleton". The resulting skeleton contained WM tracts
86 common to all subjects. Individual FA maps were then projected onto the mean FA skeleton by filling the
87 skeleton with FA values from the nearest tract center. The same non-linear transformations derived for the FA
88 maps were applied to the MD maps.

89 In terms of the LDH metric, it is a novel model-free metric that defines the regional inter-voxel coherence
90 of diffusion series (Gong 2013). Technologically, LDH is quantified within the neighbors ($n = 27$) via the
91 Kendall's coefficient concordance (KCC), after the estimation of the diffusivity strengths along each gradient
92 direction. To compare between subjects, the LDH maps were also projected onto the WM skeleton mask using
93 the TBSS framework described above. In addition, we used the same approach with different neighbor size
94 (i.e., $n = 7$ and $n = 19$) for quantifying the LDH (see Discussion), and also used another approach for
95 quantifying the regional coherence with information theory (Kong et al., 2014b) (data not shown). The results
96 in these cases were all similar to those of the original LDH.

97 The DW-MRI data preprocessing and TBSS analysis pipelines were both implemented using Nipype
98 (Gorgolewski et al. 2011), a flexible, lightweight and extensible neuroimaging data processing framework in
99 python. The pipeline for calculating both original and improved LDH was implemented in python.

100 **Assessment of in-scanner head motion**

101 To retrospectively estimate head motion during scanning, DW images were realigned to the non-DW image
102 with FMRIB's Linear Image Registration Tool (FLIRT), and at the same time, a rigid transformation matrix was
103 obtained for each image. Then for each image, the root-mean-square (RMS) deviation, which summarizes 6
104 translations and rotations across 3 axes, was calculated from 2 transformations of consecutive images
105 (Jenkinson et al. 2002). That is, in-scanner head motion was measured as the summary measure of both
106 translations and rotations of each brain volume relative to the preceding one as the previous studies
107 (Satterthwaite et al. 2012; Van Dijk et al. 2012). Finally, head motion was calculated by averaging the RMS
108 deviations for all volumes.

109 **Test-retest reliability of diffusion metrics and head motion estimate**

110 The voxel-wise test-retest reliability for each diffusion metric was calculated with the intra-class correlation
111 coefficient (ICC) (Shrout & Fleiss 1979).

$$ICC = \frac{BMS - EMS}{BMS + (k - 1) EMS}$$

112 The formula estimates the correlation of the subject signal intensities between sessions, modeled by a two-
113 way ANOVA, with random subject effects and fixed session effects. In this model, the total sum of squares is
114 split into subject (BMS), session (JMS) and error (EMS) sums of squares; the k is the number of repeated
115 sessions. The reliability measure for whole-brain analysis was implemented in python and can be accessed
116 from Nipype (Gorgolewski et al. 2011). The test-retest reliability for head motion estimate was also calculated
117 with ICC.

118 **Relationship between In-Scanner Head Motion and Diffusion Metrics**

119 To maximize the signal to noise ratio of head motion estimates, first we calculated the average head motion for
120 each participant across two sessions. Analogously, for accurate measures of microstructure estimates, the MD,
121 FA and LDH metrics finally used were also taken from the average of the TBSS results across the two sessions.
122 To examine the possible relationship between head motion and diffusion regional metrics, we conducted a
123 statistical analysis using general linear models (GLMs), for the three metrics respectively, with head motion as
124 the variable of interest. In these models, gender, age and handedness were controlled as confounding
125 covariates. Handedness was included here because it is associated with brain structure and the neural
126 processing of attention, while attention deficit may cause more head motion (e.g., Schmidt et al., 2013; Kong et
127 al., 2014a). Voxel-wise statistical analysis was performed with Threshold-Free Cluster Enhancement (TFCE)
128 correction (Smith & Nichols 2009) for multiple comparisons, considering fully corrected p-value < 0.05 as
129 significant. In addition, the same statistical procedure was conducted for both session 1 and session 2
130 respectively.

131 **Results**

132 **Test-retest reliability of diffusion metrics and head motion estimate**

133 All of the diffusion metrics in this study showed relatively high test-retest reliability: FA: Mean ICC = 0.71;
134 MD: Mean ICC = 0.71; LDH: Mean ICC = 0.75. In addition, the magnitude of head motion seemed acceptable
135 (mean = 1.18 mm, SD = 0.29; Table 1) and showed medium reliability (ICC = 0.54), which is consistent with
136 previous studies (Van Dijk et al. 2012). Although all of the diffusion metrics, as well as the head motion
137 estimate, are relatively reliable across the two scans, they were not exactly the same due to some random
138 artifacts, including motion artifacts and machine noises. Thus, for accurate measures of this microstructure and
139 the head motion estimate, we first averaged the head motion and diffusion metrics across the two sessions and
140 mainly examined the results with the averaged data.

141 ---insert Table 1. ---

142 **Relationship between the head motion estimate and diffusion metrics**

143 In Table 1, we also show a basic summary of the main results of motion effects in three diffusion metrics.

144 Among the two mostly commonly used regional diffusion metrics (i.e., FA and MD), these results
145 indicated that head motion was mainly associated with the MD values. The degree of head motion was
146 positively associated with increased MD mainly within white matter tracts in left hemisphere, including
147 anterior limb of internal capsule, posterior limb of internal capsule, genu of corpus callosum and body of
148 corpus callosum (Fig. 1). In the current report, we focus on voxels that survived the TFCE correction ($p < 0.05$)
149 (Smith & Nichols 2009) within the whole white matter skeleton. For the analyses examining FA, no voxel
150 survived correction for multiple comparisons.

151 For the analyses examining the inter-voxel diffusion metric (i.e., LDH), we found that wide-spread white
152 matter showed significant negative association with head motion ($p < 0.05$, TFCE corrected; Fig. 1). This
153 association mainly involved the bilateral superior longitudinal fasciculus, body and genu of corpus callosum,
154 cingulum, superior, anterior and posterior corona radiate, retrolenticular part of internal capsule, fornix,
155 cerebral peduncle, middle cerebellar peduncle, right anterior and posterior limb of internal capsule, right
156 external capsule and sagittal stratum.

157 ---insert Fig. 1. ---

158 Overall, with the same criterion of significance ($p < 0.05$, TFCE corrected), we found the most number of
159 motion-related voxels with LDH (34551 voxels, 32.25%) and then MD (2686 voxels, 2.51%). No voxel
160 survived with FA.

161 In addition, we also examined the association between head motion and diffusion metrics with data from
162 the two sessions respectively. Although no voxel survived statistical correction for multiple comparisons ($p <$
163 0.05) in most of the analyses (except LDH in Session 2), there were some voxels that showed a significant
164 trend ($p < 0.10$, TFCE corrected; Fig. 2).

165 ---insert Fig. 2. ---

166 Discussion

167 Like any other MRI technique, DW-MRI signal is subject to head motion artifacts, however, the relationship
168 between diffusion metrics and head motion remains incompletely understood. Previous studies have shown a
169 significant relationship between diffusion metrics and head motion (Ling et al. 2012) with conventional
170 scanning protocol. The current study expands on previous work by exploring the relationship between motion
171 and diffusion metrics (including the recently proposed inter-voxel metric, LDH) with a multiband dataset. We
172 found that the motion effects in FA and MD seems to be mitigated to some extent, but the effect on MD still
173 existed. In addition, the effect is much more pronounced in LDH. Since these results are present following
174 standard processing procedures, researchers shall be cautious when conducting data analysis and interpretation.

175 Previous studies suggested a positive association between motion and MD, with increased magnitude of MD
176 as a result of increased total motion (Ling et al. 2012). The results of this study, with multiband dataset,
177 replicate this finding, as a positive relationship between head motion and the magnitude of MD was present in
178 the left hemisphere tracts. The significant association was mainly located in the deeper white matter (e.g.,
179 corpus callosum and the internal capsule). Interestingly, these tracts have often been reported in the literature to
180 differ between a variety of clinical populations and healthy subjects (Carrasco et al. 2012; Travers et al. 2012).
181 For examining FA, we found no significant relationship between head motion and FA after multiple comparison
182 correction. On the one hand, our findings appear consistent with the previous finding (Ling et al., 2012) that the
183 head motion's bias is more pronounced in MD than FA. But on the other hand, given the reduction of the
184 number of motion-related voxels (multiband dataset: 0 voxel for FA, 2686 voxels for MD; Ling et al., (2012):
185 2422 voxels for FA, 22679 voxels for MD), the motion effect seems to be mitigated in the multiband dataset.
186 This may be due to several advantages of the multiband dataset. First, the multiband dataset was acquired with

187 much more gradient directions than traditional datasets, which would result in more accuracy when evaluating
188 diffusion metrics. Second, the multiband scanning protocol allows full-brain coverage through the acquisition
189 of multiple slices simultaneously. This could avoid displacements of brain within a TR and further mitigate the
190 motion effects. Finally, given the fact that multiband protocol is designed for a relatively high sampling rate
191 (i.e., a shorter TR), motion effects from a shorter duration would be expected to decrease. All these advantages
192 could result in higher accuracy and less irrelevant effects (e.g., head motion) when evaluating diffusion metrics.

193 In addition, we also explored the relationship between head motion and LDH values and found that there
194 were widespread voxels significantly associated to head motion. It's worth noting that with a smaller neighbor
195 sizes ($n = 19$ or $n = 7$) when calculating the LDH, we observed the similar result (number of voxels that
196 survived the TFCE correction: 35570 voxels for $n = 19$; 40425 voxels for $n = 7$). This appears to be quite likely
197 caused by motion artifacts. Indeed, the significant voxels were rarely located in the occipital white matter
198 tracts, where motion artifacts may be much weaker than that in prefrontal lobe when subjects are laying supine.
199 These results suggest that LDH values might be more subject to head motion artifacts. The increased
200 susceptibility to motion may be due to the fact that it is an inter-voxel metric which would be subject to shear in
201 the displacement, and that it is directly calculated with raw diffusivity series. Though previous studies have
202 shown LDH values change during aging, the newly proposed metric has not yet well validated (Gong 2013)
203 and simulation and experimental work is required to confirm the motion-LDH association.

204 So, why does the association between motion and diffusion metrics exist? The dominant view at present is
205 that head motion introduces artifacts into diffusion signals, similar to what has been noted in the fMRI
206 literature (Bullmore et al. 1999; Friston et al. 1996; Hajnal et al. 1994), which influence the calculation of
207 diffusion metrics and further results of cross-subject analysis. A common strategy for controlling motion effects
208 in neuroimaging cross-subject analysis is to regress or match motion estimates (Zuo et al. 2010a; Zuo et al.
209 2012; Zuo et al. 2010b). Another strategy for mitigating head-motion artifacts is to remove time series of high
210 motion, which is called 'scrubbing' (Power et al. 2012). However, these strategies have their limitations. On the
211 one hand, scrubbing volumes with high motion could not fundamentally change the relationship between
212 motion and values of diffusion metrics (Ling et al. 2012). On the other hand, they may also reduce the ability to
213 detect a significant effect of interest, and/or introduce sampling bias (Satterthwaite et al. 2012; Wylie et al.
214 2014).

215 While researchers attempt to propose more sophisticated algorithms, there is growing perception in the
216 field that head motion reflects individual differences in psychological traits and clinical conditions. For
217 instance, previous studies showed that head motion was correlated with some psychological and clinical

218 measures, such as the autism symptom severity score (Yendiki et al. 2013). In addition, previous fMRI studies
219 suggest that the association may reflect the neural processing related to head motion (Yan et al. 2013a; Yan et
220 al. 2013b). However, it is important to note that this problem in dMRI would not be as serious as it is in fMRI,
221 since in dMRI the structures affected by motion are not necessarily the one reflecting the motion processing.
222 Nevertheless, these findings do suggest that head motion might not just a random variable.

223 Taken together, as articulated previously (Van Dijk et al. 2012; Wylie et al. 2014; Yendiki et al. 2013),
224 these findings demonstrate the significance of developing motion-compensated acquisition methods for DW-
225 MRI and incorporating them into neuroimaging studies in the future. Nevertheless, with current technologies, it
226 appears impossible to perfectly eliminate the motion effects. As a temporary solution, examining both models
227 with and without motion being regressed out will be expected. But in this case, researcher should include both
228 results in the report, rather than just pick a 'better' one. Additionally, researcher shall keep in mind that motion
229 does not only influence MRI signals, but also correlated with some meaningful individual differences.
230 Alternatively, replication in an independent sample would be helpful, since the effects of head motion on
231 diffusion metrics are usually random and not specific to some brain regions. Nevertheless, for now, researchers
232 shall be cautious when doing MRI data analysis and interpretation.

233 In sum, the results of this study indicate that, in the multiband diffusion data, there are also significant
234 associations between head motion and diffusion metrics, although the motion effects appear to be mitigated
235 compared to those with traditional dataset. Specifically, head motion was associated with both MD and LDH,
236 and no significant effect was found for FA. Future studies should investigate the association between head
237 motion and diffusion metrics with larger multiband datasets.

238 **References**

- 239 Bullmore ET, Brammer MJ, Rabe-Hesketh S, Curtis VA, Morris RG, Williams SC, Sharma T, and
240 McGuire PK. 1999. Methods for diagnosis and treatment of stimulus-correlated motion in generic brain
241 activation studies using fMRI. *Hum Brain Mapp* 7:38-48.
- 242 Carrasco JL, Tajima-Pozo K, Diaz-Marsa M, Casado A, Lopez-Ibor JJ, Arrazola J, and Yus M. 2012.
243 Microstructural white matter damage at orbitofrontal areas in borderline personality disorder. *J Affect*
244 *Disord* 139:149-153.
- 245 Friston KJ, Williams S, Howard R, Frackowiak RS, and Turner R. 1996. Movement-related effects in
246 fMRI time-series. *Magn Reson Med* 35:346-355.
- 247 Golby AJ, Kindlmann G, Norton I, Yarmarkovich A, Pieper S, and Kikinis R. 2011. Interactive
248 diffusion tensor tractography visualization for neurosurgical planning. *Neurosurgery* 68:496-505.
- 249 Gong G. 2013. Local diffusion homogeneity (LDH): an inter-voxel diffusion MRI metric for assessing
250 inter-subject white matter variability. *PLoS One* 8:e66366.
- 251 Gong G, He Y, Concha L, Lebel C, Gross DW, Evans AC, and Beaulieu C. 2009. Mapping anatomical
252 connectivity patterns of human cerebral cortex using in vivo diffusion tensor imaging tractography. *Cereb*
253 *Cortex* 19:524-536.
- 254 Gorgolewski K, Burns CD, Madison C, Clark D, Halchenko YO, Waskom ML, and Ghosh SS. 2011.
255 Nipype: a flexible, lightweight and extensible neuroimaging data processing framework in python. *Front*
256 *Neuroinform* 5:13.
- 257 Hajnal JV, Myers R, Oatridge A, Schwieso JE, Young IR, and Bydder GM. 1994. Artifacts due to
258 stimulus correlated motion in functional imaging of the brain. *Magn Reson Med* 31:283-291.
- 259 Jenkinson M, Bannister P, Brady M, and Smith S. 2002. Improved optimization for the robust and
260 accurate linear registration and motion correction of brain images. *Neuroimage* 17:825-841.
- 261 Johansen-Berg H. 2010. Behavioural relevance of variation in white matter microstructure. *Curr Opin*
262 *Neurol* 23:351-358.
- 263 Kong XZ. 2014a. Head motion in children with ADHD during resting-state brain imaging. *PeerJ*
264 *PrePrints* 2.
- 265 Kong XZ, Zhen Z, Liu J. 2014b. Measuring Regional Diffusivity Dependency via Mutual Information.
266 *Presented at the IEEE International Symposium on Biomedical Imaging*. April 29-May 2. 2014. Beijing.
267 China.
- 268 Landman BA, Farrell JA, Jones CK, Smith SA, Prince JL, and Mori S. 2007. Effects of diffusion
269 weighting schemes on the reproducibility of DTI-derived fractional anisotropy, mean diffusivity, and
270 principal eigenvector measurements at 1.5T. *Neuroimage* 36:1123-1138.
- 271 Le Bihan D. 2003. Looking into the functional architecture of the brain with diffusion MRI. *Nat Rev*
272 *Neurosci* 4:469-480.
- 273 Le Bihan D, Mangin JF, Poupon C, Clark CA, Pappata S, Molko N, and Chabriat H. 2001. Diffusion
274 tensor imaging: concepts and applications. *J Magn Reson Imaging* 13:534-546.
- 275 Ling J, Merideth F, Caprihan A, Pena A, Teshiba T, and Mayer AR. 2012. Head injury or head motion?
276 Assessment and quantification of motion artifacts in diffusion tensor imaging studies. *Hum Brain Mapp*
277 33:50-62.
- 278 Mennes M, Biswal BB, Castellanos FX, and Milham MP. 2012. Making data sharing work: The
279 FCP/INDI experience. *Neuroimage*.

- 280 Moeller S, Yacoub E, Olman CA, Auerbach E, Strupp J, Harel N, and Ugurbil K. 2010. Multiband
281 multislice GE-EPI at 7 tesla, with 16-fold acceleration using partial parallel imaging with application to
282 high spatial and temporal whole-brain fMRI. *Magn Reson Med* 63:1144-1153.
- 283 Power JD, Barnes KA, Snyder AZ, Schlaggar BL, and Petersen SE. 2012. Spurious but systematic
284 correlations in functional connectivity MRI networks arise from subject motion. *Neuroimage* 59:2142-2154.
- 285 Satterthwaite TD, Wolf DH, Loughhead J, Ruparel K, Elliott MA, Hakonarson H, Gur RC, and Gur RE.
286 2012. Impact of in-scanner head motion on multiple measures of functional connectivity: relevance for
287 studies of neurodevelopment in youth. *Neuroimage* 60:623-632.
- 288 Schmidt SL, Simões EN, Schmidt GJ. 2013. The Effects of Hand Preference on Attention. *Psychology*
289 4: 29-33.
- 290 Shrout PE, and Fleiss JL. 1979. Intraclass correlations: uses in assessing rater reliability. *Psychol Bull*
291 86:420-428.
- 292 Smith SM, Jenkinson M, Johansen-Berg H, Rueckert D, Nichols TE, Mackay CE, Watkins KE,
293 Ciccarelli O, Cader MZ, Matthews PM, and Behrens TE. 2006. Tract-based spatial statistics: voxelwise
294 analysis of multi-subject diffusion data. *Neuroimage* 31:1487-1505.
- 295 Smith SM, Jenkinson M, Woolrich MW, Beckmann CF, Behrens TEJ, Johansen-Berg H, Bannister PR,
296 De Luca M, Drobnjak I, Flitney DE, Niazy RK, Saunders J, Vickers J, Zhang YY, De Stefano N, Brady JM,
297 and Matthews PM. 2004. Advances in functional and structural MR image analysis and implementation as
298 FSL. *Neuroimage* 23:S208-S219.
- 299 Smith SM, Johansen-Berg H, Jenkinson M, Rueckert D, Nichols TE, Miller KL, Robson MD, Jones
300 DK, Klein JC, Bartsch AJ, and Behrens TE. 2007. Acquisition and voxelwise analysis of multi-subject
301 diffusion data with tract-based spatial statistics. *Nat Protoc* 2:499-503.
- 302 Smith SM, and Nichols TE. 2009. Threshold-free cluster enhancement: addressing problems of
303 smoothing, threshold dependence and localisation in cluster inference. *Neuroimage* 44:83-98.
- 304 Tijssen RH, Jansen JF, and Backes WH. 2009. Assessing and minimizing the effects of noise and
305 motion in clinical DTI at 3 T. *Hum Brain Mapp* 30:2641-2655.
- 306 Travers BG, Adluru N, Ennis C, Tromp do PM, Destiche D, Doran S, Bigler ED, Lange N, Lainhart
307 JE, and Alexander AL. 2012. Diffusion tensor imaging in autism spectrum disorder: a review. *Autism Res*
308 5:289-313.
- 309 Van Dijk KR, Sabuncu MR, and Buckner RL. 2012. The influence of head motion on intrinsic
310 functional connectivity MRI. *Neuroimage* 59:431-438.
- 311 Wylie GR, Genova H, Deluca J, Chiaravalloti N, and Sumowski JF. 2014. Functional magnetic
312 resonance imaging movers and shakers: Does subject-movement cause sampling bias? *Hum Brain Mapp*
313 35:1-13.
- 314 Yan C-G, Craddock RC, He Y, and Milham MP. 2013a. Addressing Head Motion Dependencies for
315 Small-World Topologies in Functional Connectomics. *Frontiers in Human Neuroscience* 7:910.
- 316 Yan CG, Cheung B, Kelly C, Colcombe S, Craddock RC, Di Martino A, Li Q, Zuo XN, Castellanos
317 FX, and Milham MP. 2013b. A comprehensive assessment of regional variation in the impact of head
318 micromovements on functional connectomics. *Neuroimage*.
- 319 Yendiki A, Koldewyn K, Kakunoori S, Kanwisher N, and Fischl B. 2013. Spurious group differences
320 due to head motion in a diffusion MRI study. *Neuroimage*.

- 321 Zahneisen B, Grotz T, Lee KJ, Ohlendorf S, Reisert M, Zaitsev M, and Hennig J. 2011. Three-
322 dimensional MR-encephalography: fast volumetric brain imaging using rosette trajectories. *Magn Reson*
323 *Med* 65:1260-1268.
- 324 Zuo XN, Di Martino A, Kelly C, Shehzad ZE, Gee DG, Klein DF, Castellanos FX, Biswal BB, and
325 Milham MP. 2010a. The oscillating brain: complex and reliable. *Neuroimage* 49:1432-1445.
- 326 Zuo XN, Ehmke R, Mennes M, Imperati D, Castellanos FX, Sporns O, and Milham MP. 2012.
327 Network centrality in the human functional connectome. *Cereb Cortex* 22:1862-1875.
- 328 Zuo XN, Kelly C, Di Martino A, Mennes M, Margulies DS, Bangaru S, Grzadzinski R, Evans AC,
329 Zang YF, Castellanos FX, and Milham MP. 2010b. Growing together and growing apart: regional and sex
330 differences in the lifespan developmental trajectories of functional homotopy. *J Neurosci* 30:15034-15043.
- 331

Table 1 (on next page)

A basic summary of head motion and the motion effects in three diffusion metrics.

The column Motion includes the averaged motion in the sample. The column Motion-Brain Association includes the summary of motion effects in different diffusion metrics (i.e., FA, MD, and LDH). n.r. indicates null results; Plus sign (+) indicates a positive relationship, while minus (–) indicates a negative relationship. *: $p < 0.10$ TFCE corrected, **: $p < 0.05$ TFCE corrected.

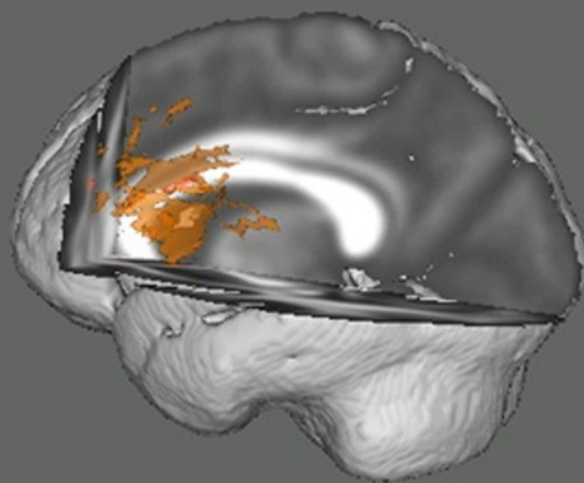
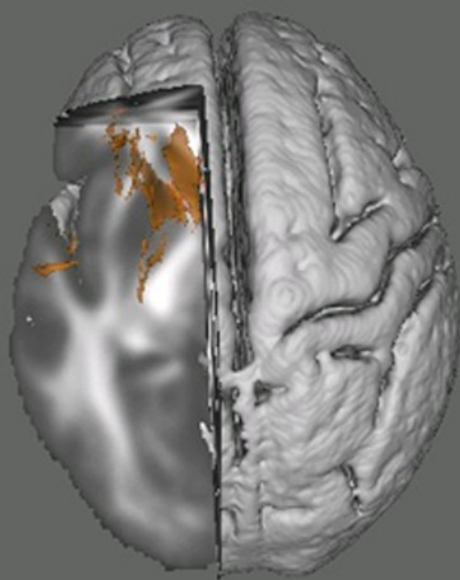
Sample	Motion	Motion-Brain Association		
		FA	MD	LDH
Session 1	1.1(0.32)	n.r.	+*	-*
Session 2	1.26(0.38)	n.r.	+*	-**
Averaged	1.18(0.29)	n.r.	+**	-**

Figure 1

Results from the tract-based spatial statistics (TBSS) analyses depicting the voxels that showed a significant association between head motion diffusion metrics.

Data are presented for the analyses involving both Mean Diffusivity (MD; A) and local diffusion Local Diffusion Homogeneity (LDH; B) as the dependent measure. Participants with higher motion exhibited higher apparent values of MD, but lower LDH. Voxels survived the TFCE correction ($p < 0.05$) across the whole white matter skeleton are displayed.

MD



LDH

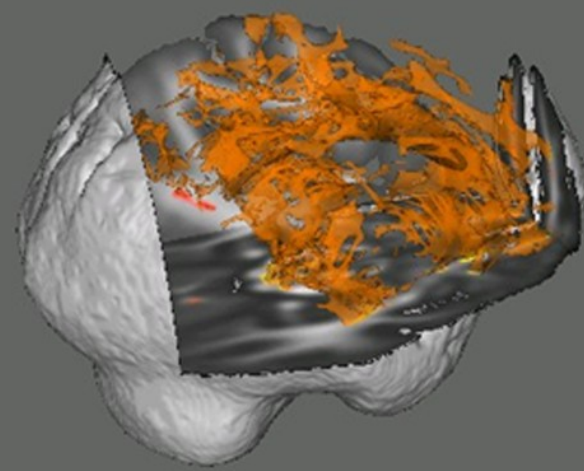
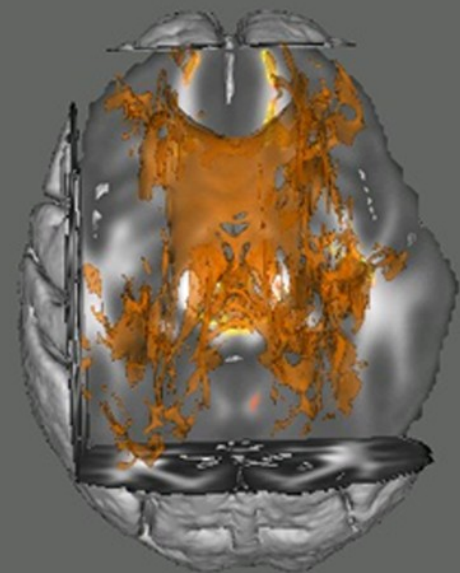


Figure 2

Results from the tract-based spatial statistics (TBSS) analyses depicting the voxels that showed a significant association between head motion diffusion metrics.

Since no voxel that survived statistical correction for multiple comparisons ($p < 0.05$) in most of the analyses (except LDH in Session 2), they are displayed at a more tolerant threshold ($p < 0.10$, TFCE corrected).

